


Nonlinear Optics Hot Paper

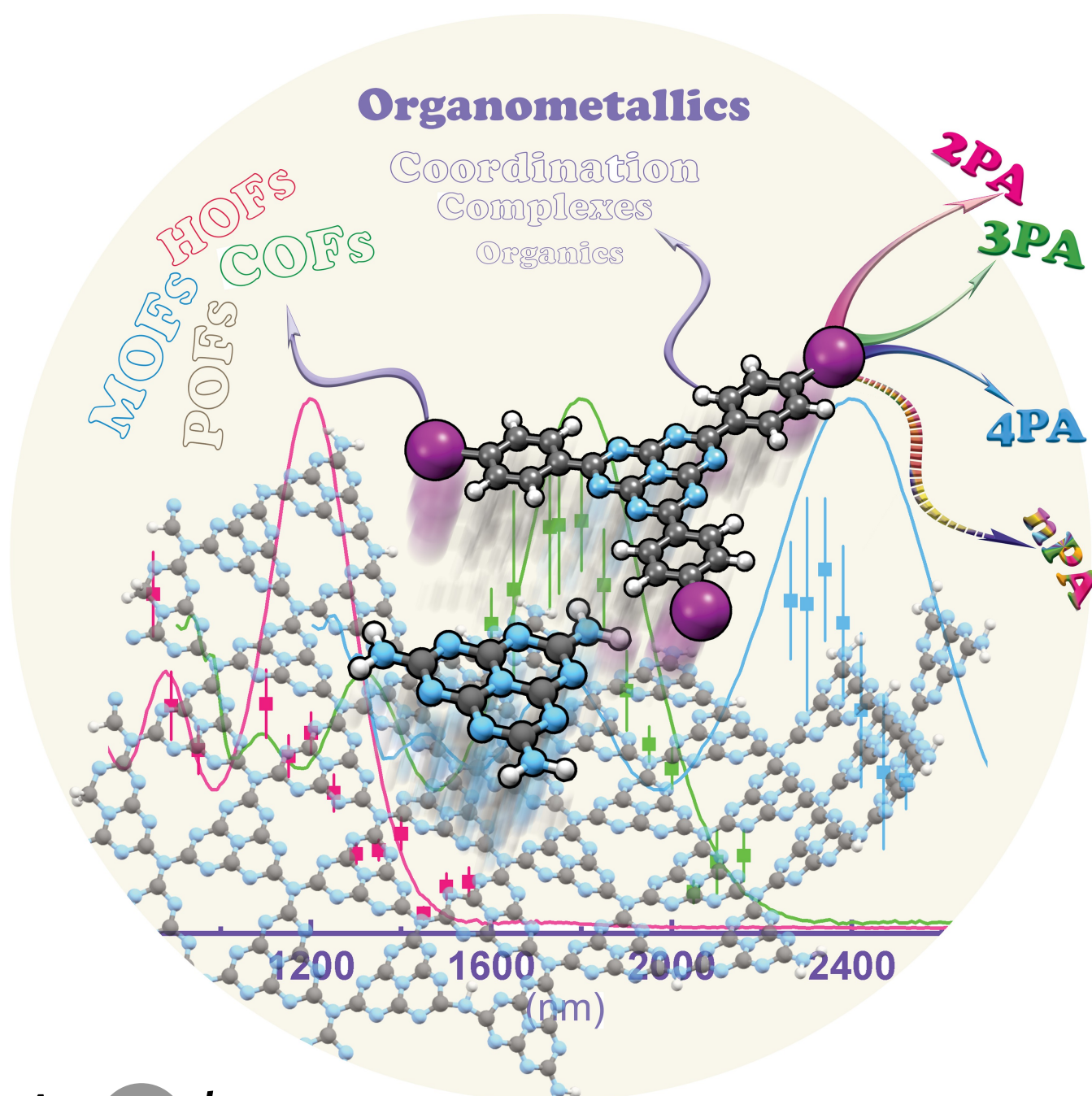
 How to cite: *Angew. Chem. Int. Ed.* **2022**, *61*, e202208168

International Edition: doi.org/10.1002/anie.202208168

German Edition: doi.org/10.1002/ange.202208168

Giant Multi-Photon Absorption by Heptazine Organometalation

Ling Zhang, Mahbod Morshedi, Mahesh S. Kodikara, and Mark G. Humphrey*

 Dedicated to Professor Glen B. Deacon on the occasion of his 85th birthday


Abstract: Multi-photon absorption (MPA) is of increasing interest for applications in technologically important “windows” of the electromagnetic spectrum (near-infrared III, NIR-III, 1550–1870 nm; and the new 2080–2340 nm region); however, few molecules exist that display strong MPA at these long wavelengths. We herein report the syntheses of the first 2,5,8-*s*-heptazine-cored organometallic complexes, together with organic analogues. The complexes exhibit outstanding 3PA cross-sections in the NIR-III and exceptional 4PA cross-sections in the new 2080–2340 nm window. We demonstrate that replacing organic donor groups by organometallic units results in an order of magnitude increase in 3PA, the “switching on” of 4PA, and a dramatic improvement in photo-stability. Our results highlight the impressive outcomes possible with an “organometalation” approach to NLO materials design.

Multi-photon absorption (MPA) is a nonlinear optical (NLO) effect that is attracting significant attention for use in applications that necessitate precise control of interaction volume, e.g., micromachining, biological imaging, and targeted therapy. For many applications, MPA efficiency is particularly desirable in certain key technologically-important wavelength ranges, such as the telecom windows at which the transparency of silica is maximized (1260–1675 nm) and the biological windows at which the transparencies of tissue and other biological media are maximized (near-infrared I, NIR-I: 650–950 nm; NIR-II: 1000–1350 nm; NIR-III: 1550–1870 nm).^[1] The vast majority of MPA studies have focused on two-photon absorption (2PA), for which structure–property relationships have afforded insight into the factors that favorably impact on 2PA merit.^[2] Most molecules exhibit maximal 2PA at wavelengths close to twice the wavelength of intense linear optical absorption (1PA) bands, and this is usually at comparatively short wavelengths (in the NIR-I and occasionally in the NIR-II region). As a result, there is a strong contemporary need to develop MPA materials with suitable performance at NIR-III and at longer wavelength regions such as the newly-proposed 2080–2340 nm window.^[3] This increasing interest in longer wavelength MPA has encouraged studies of higher-order *n*PA ($n > 2$), with a significant number of 3PA reports and an increasing number of studies

of 4PA.^[4] Indeed, recent reports have disclosed 5PA and 6PA in both the NIR-III and the new 2080–2340 nm windows.^[5–7] However, such higher-order MPA effects are intrinsically weaker than lower-order MPA, and molecules that exhibit strong MPA efficiency at long wavelengths remain rare.

The foregoing discussion suggests that the pursuit of MPA materials that can operate at NIR-III and longer wavelengths should ideally exploit lower-order MPA, and that consequently the focus should shift to molecules that possess longer-wavelength 1PA bands. Strong donor-acceptor (D-A) intramolecular charge-transfer (CT) interactions are often associated with longer-wavelength optical absorption bands and strong NLO effects, particularly in instances where the donor group is an electron-rich ligated metal.^[8] In the search for a flexible and efficient electron-accepting moiety that can be used in D_nA constructs, we noted that *s*-heptazine (IUPAC preferred name: 1,3,3a¹,4,6,7,9-heptaaza-phenalene) is an intriguing possible core in formally octupolar D_3A stars, due to its electronegative N-rich composition and planar fully conjugated structure rendering it a highly efficient acceptor.^[9] Surprisingly, there have been no organometallic *s*-heptazine derivatives reported thus far, and there have been no higher-order NLO studies of heptazine derivatives.^[10,11] We report herein i) the design, synthesis, and characterization of a novel triethynyl-*s*-heptazine precursor that is a potential candidate for the efficient synthesis of N-rich carbon nitride network materials, ii) the tailored synthesis of new 2,5,8-tri(donor)-*s*-heptazines, including the first organometallic examples, iii) NLO studies examining the MPA performance of the new organic and organometallic heptazines towards femtosecond light pulses over a broad spectral range spanning the NIR and the aforementioned key technological “windows”, iv) identification of outstanding molecular 3PA in the NIR-III and at longer wavelengths, v) observation of exceptional molecular 4PA in the newly-identified 2080–2340 nm window, vi) an order of magnitude improvement in 3PA/4PA cross-sections in progression from amino to organometallic donor, coupled to dramatic improvements in photo-stability, and vii) computational studies that have facilitated assignment of the linear optical transitions, and suggested the origin of the impressive MPA behavior.

Figure 1 shows the *s*-heptazine-cored compounds in this study. All new compounds possess a D_3A composition in which the donor groups are bis-{bis(diphenylphosphino)ethane}ruthenium units with *trans*-disposed alkynyl/chlorido ligands or alkyne-functionalized *p*-anilino groups. The syntheses proceeded by Friedel–Crafts arylation of 2,5,8-trichloro-*s*-heptazine with anisole, conversion of the resultant tri(1,4-anisyl)-substituted compound to tri(1,4-hydroxyphenyl)- and then tri(1,4-triflatophenyl)- derivatives, and then Sonogashira coupling of the tri(triflato) compound with ethynyltrimethylsilane to afford the key 2,5,8-tris(1,4-trimethylsilylethynylphenyl)-*s*-heptazine derivative. This polycyclic quasi-planar heptazine is photoluminescent and possesses excellent solubility, making it an attractive potential precursor to metal–organic frameworks (MOFs) and covalent organic frameworks (COFs) following

[*] Dr. L. Zhang, Dr. M. Morshedi, Prof. M. G. Humphrey
Research School of Chemistry, Australian National University
Canberra, ACT 2601 (Australia)
E-mail: Mark.Humphrey@anu.edu.au

Dr. M. S. Kodikara
Department of Chemistry, University of Ruhuna
Matara, 81000 (Sri Lanka)

© 2022 The Authors. Angewandte Chemie International Edition published by Wiley-VCH GmbH. This is an open access article under the terms of the Creative Commons Attribution Non-Commercial NoDerivs License, which permits use and distribution in any medium, provided the original work is properly cited, the use is non-commercial and no modifications or adaptations are made.

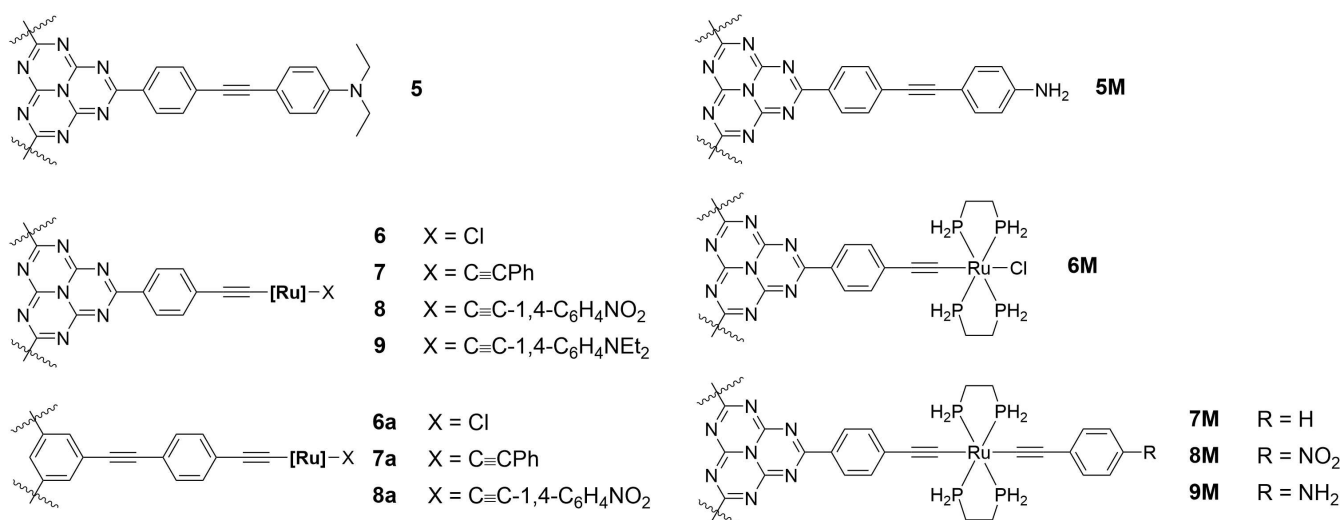


Figure 1. Compounds in this study (new compounds **5–9**, previously reported complexes **6a–8a**, computational models **5M–9M**). [Ru]: *trans*-[Ru(κ^2 -dppe)₂] (dppe = 1,2-bis(diphenylphosphino)ethane). Wavy lines: equivalent arms at central heptazine or benzene cores.

in situ desilylation. The desilylation of this trimethylsilylethynyl derivative afforded the tri(ethynyl) intermediate to which the organic and organometallic donor units were coupled. Complete synthetic and spectroscopic characterization details, as well as ¹H, ¹³C, and ³¹P NMR spectra confirming the identity of the new compounds and their precursors, and electrospray ionization time-of-flight mass spectrometry data confirming the identity of the chloride-containing organometallic **6** (Figures S1–S26, Table S1), are collected in the Supporting Information.

The UV/Vis spectra of **5–9** are provided in the Supporting Information (Figure S27), with the key bands assigned by time-dependent density functional theory (TD-DFT) calculations (Figures S38–S43 and Tables S7 and S8). The UV/Vis spectrum of the *N,N*-diethylanilino derivative **5** exhibits a strong band at 508 nm assigned to an admixture of LUMO←HOMO and LUMO←HOMO-1, and corresponding to charge transfer from the peripheral anilinoethynyl units to the heptazine core. The UV/Vis spectra of the organometallic derivatives **6–9** show more intense bands in the range 583–616 nm assigned to admixtures of LUMO←HOMO and LUMO←HOMO-1, corresponding to charge transfer from the *trans*-[Ru(C≡C)X(L₂)₂] groups to the heptazine core, and with an increased X contribution for X = anilinoethynyl.

The nonlinear absorption and nonlinear refraction properties of **5–9** were measured using open-aperture and closed-aperture Z-scan experiments over the spectral range 800–2520 nm, and using ca. 130 femtosecond pulses (Figures S28–S32). The absorptive nonlinearities have been replotted as the corresponding multi-photon absorption cross-sections; these are presented in Figure 2 and Figures S28–S32, and we have also included the linear optical absorption spectra, plotted at two- to four-times the wavelength, to provide an eye-guide and facilitate interpretation. Compounds **5–9** show nonlinear absorption maxima at ca. 1100–1150 nm, 1600–1750 nm, and (in the case of **6–9**) 2100–

2300 nm, confirmed to be 2PA, 3PA, and 4PA in nature, respectively, from the intensity dependencies of the corresponding open-aperture fs Z-scan traces (see Figures S33–S35 for the intensity-dependence traces of **9**). It is particularly noteworthy that the wavelengths of the maximal values of the intensity dependence-assigned MPA for **6–9** correspond closely to the (slightly blue-shifted) appropriate multiples of the wavelength of the lowest-energy metal-to-heptazine charge-transfer band. We also note that, while the organic derivative **5** showed evidence for instability during extended Z-scan studies, the organometallic complexes **6–9** displayed photo-stability under these conditions (Figures S36, S37); organometalation therefore results in a significant improvement in the resistance to photo-degradation by high-intensity light.

Linear and nonlinear absorption data for **5–9** are collected in Tables 1 and S5, together with data for the previously reported 1,3,5-benzene-cored analogues **6a–8a** that are depicted in Figure 1. The 2PA cross-section increases slightly on proceeding from organic **5** to chlorido-ligated **6**, and then increases significantly on progressing to **7–9**. The increase in 3PA cross-section is more dramatic, maximal values for **6–9** being an order of magnitude greater than that for **5**. The organometallics display 4PA, in contrast to organic **5** which is inactive in the corresponding wavelength range. Complex **9**, incorporating an electron-donating 4-(*N,N*-diethylamino)phenylethynyl ligand, is the most efficient multi-photon absorber across this series of complexes. The improvements in MPA performance that are seen on replacing 1,3,5-triethynylbenzene with heptazine core are profound, significant increases in maximal values and dramatic red-shifts in maxima being observed. To effect a more rigorous comparison, we also explored scaling the maximal values by molecular weight (which is the most common procedure to compare molecules), as well as by the appropriate power of the “number of effective electrons”; the latter is a theoretically precise approach that considers

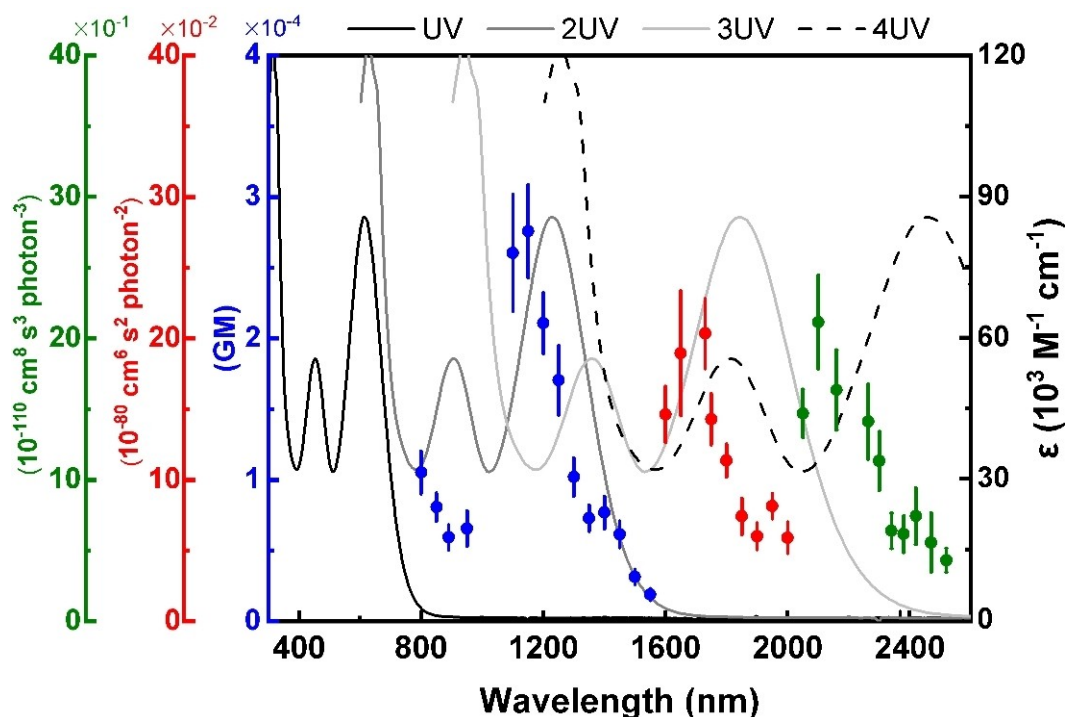


Figure 2. Wavelength dependence of the nonlinear absorption of **9**. Plots of σ_2 (blue), σ_3 (red), and σ_4 (green) overlaid on the UV/Vis spectrum (black), and including plots of the UV/Vis spectrum as a function of twice (dark grey), three times (light grey), and four times (dashes) the wavelength.

Table 1: Linear optical and NLO absorption cross-section maxima, and MWT- and number of “effective” electrons-scaled σ_n data ($n=2-4$).^[a]

| Complex | $\lambda_{1,max}^{[b]}$ [nm] ^[c] | $\lambda_{2,max}^{[b]}$ [nm] ^[c] | $\sigma_2^{[d]}$ ($\lambda_{max}^{[b]}$) | $\sigma_2/M_1^{[e]}$ σ_2/N_{eff}^2 [d,f] ($\lambda_{max}^{[b]}$) | $\sigma_3^{[g]}$ ($\lambda_{max}^{[b]}$) | $\sigma_3/M_1^{[h]}$ σ_3/N_{eff}^3 [d] ($\lambda_{max}^{[b]}$) | $\sigma_4^{[i]}$ ($\lambda_{max}^{[b]}$) | $\sigma_4/M_1^{[j]}$ σ_4/N_{eff}^4 [d] ($\lambda_{max}^{[b]}$) |
|-----------|---|---|--|---|--|---|--|---|
| 5 | 508 [50] | – | 2760 (1150) | 3.02, 2.84 (1150) | 120 (1650) | 0.13, 0.0040 (1650) | ^[k] | – |
| 6 | 439 [29] | 598 [60] | 3250 (1100) | 0.99, 7.44 (1100) | 1640 (1600) | 0.50, 0.18 (1600) | 110 (2300) | 0.034, 0.00058 (2300) |
| 7 | 433 [60] | 601 [102] | 16040 (1100) | 4.63, 25.46 (1100) | 1150 (1600) | 0.33, 0.073 (1600) | 100 (2260) | 0.029, 0.00025 (2260) |
| 8 | 463 [75] | 583 [114] | 13780 (1100) | 3.83, 21.87 (1100) | 1250 (1750) | 0.35, 0.078 (1750) | 160 (2260) | 0.044, 0.00040 (2260) |
| 9 | 454 [56] | 616 [86] | 27580 (1150) | 7.49, 43.09 (1150) | 2030 (1730) | 0.55, 0.12 (1730) | 210 (2100) | 0.057, 0.00051 (2100) |
| 6a | 413 [9.9] | – | 1050 (845) | 0.32, 2.43 (845) | 190 (1290) | 0.059, 0.021 (1290) | ^[k] | – |
| 7a | 412 [12] | – | 370 (810) | 0.11, 0.59 (810) | 100 (1240) | 0.029, 0.0064 (1240) | ^[k] | – |
| 8a | 403 [11] | 459 [8.9] | 1100 (950) | 0.31, 1.76 (950) | 740 (1290) | 0.21, 0.047 (1290) | ^[k] | – |

[a] Solvent CH_2Cl_2 . [b] nm. [c] $10^4 \text{ L mol}^{-1} \text{ cm}^{-1}$. [d] $\text{GM} = 10^{-50} \text{ cm}^4 \text{ s photon}^{-1}$. [e] GM mol g^{-1} . [f] $N_{eff} = 20.8$ (**6a**), 25.0 (**7a**), 25.0 (**8a**), 31.2 (**5**), 20.9 (**6**), 25.1 (**7**), 25.1 (**8**), 25.3 (**9**). [g] $10^{-80} \text{ cm}^6 \text{ s}^2 \text{ photon}^{-2}$. [h] $10^{-80} \text{ cm}^6 \text{ s}^2 \text{ photon}^{-2} \text{ mol g}^{-1}$. [i] $10^{-110} \text{ cm}^8 \text{ s}^3 \text{ photon}^{-3}$. [j] $10^{-110} \text{ cm}^8 \text{ s}^3 \text{ photon}^{-3} \text{ mol g}^{-1}$. [k] No measurable activity.

the polarizable electrons contributing to the nonlinear absorptive behavior^[12–14] (Tables 1 and S6). Complex **9** maintains its primacy in MPA performance across most comparators.

A key feature of complexes **6–9** is the existence of 3PA behavior in the NIR-III and 4PA behavior in the recently proposed 2080–2340 nm window. There are few reports of molecules exhibiting 3PA in the NIR-III region, particularly at wavelengths beyond 1600 nm for which the only extant examples are bis(5-*N,N*-diethylthiophene-2-terpyridine)zinc(II) ($0.117 \times 10^{-80} \text{ cm}^6 \text{ s}^2 \text{ photon}^{-2}$ @ 1700 nm, 140 fs pulses)^[15] and functionalized (tetrabenzoporphyrin)platinum(II) complexes ($(0.79\text{--}1.69) \times 10^{-80} \text{ cm}^6 \text{ s}^2 \text{ photon}^{-2}$ @ 1700–1800 nm, 100 fs pulses).^[16] Cross-sections for the present series of complexes are three orders of magnitude greater. There are no examples of molecules exhibiting 4PA activity in the

2080–2340 nm window thus far, nPA data in this region being restricted to intrinsically weaker 6PA. These complexes therefore present a dramatic improvement in MPA merit over extant literature examples in increasingly important regions of the electromagnetic spectrum.

In conclusion, we have reported the first organometallic *s*-heptazines and examined their MPA performance towards femtosecond light pulses over a spectral range spanning the NIR and key technological “windows”. We have identified outstanding molecular 3PA in the NIR-III and at longer wavelengths, with maximal values three orders of magnitude larger than previously reported molecular 3PA cross-sections in this wavelength range. We also report exceptional molecular 4PA in the newly identified 2080–2340 nm window, a region in which previous MPA reports are restricted to intrinsically weaker 5PA and 6PA. The system-

atic variation across this series of compounds has shown that both MPA activity and photo-stability improve markedly on proceeding from organic to organometallic and that MPA activity red-shifts and improves significantly on replacing 1,3,5-triethynylbenzene with heptazine core. Maximal nPA values are found at the (slightly blue-shifted) appropriate multiples of a key linear optical transition that computational studies assign as metal-to-heptazine charge-transfer in character. The present study highlights a route to photo-stable materials with outstanding MPA activity in wavelength regions of increasing technological interest.

Acknowledgements

L.Z. thanks the China Scholarship Council and the Australian National University for an ANU-CSC Postgraduate Scholarship. M.G.H. thanks the Australian Research Council for support (DP170100408, DP220100111). This work was supported by computational resources provided by the Australian Government through the National Computational Infrastructure (NCI) under the ANU Merit Allocation Scheme (project eo34). Open access publishing facilitated by Australian National University, as part of the Wiley - Australian National University agreement via the Council of Australian University Librarians.

Conflict of Interest

The authors declare no conflict of interest.

Data Availability Statement

The data that support the findings of this study are available in the Supporting Information of this article.

Keywords: Metal Complexes • Multi-Photon Absorption • Nitrogen Heterocycles • Nonlinear Optics • Organometallics

[1] E. Hemmer, A. Benayas, F. Légaré, F. Vetrone, *Nanoscale Horiz.* **2016**, *1*, 168–184.

- [2] G. S. He, L.-S. Tan, Q. Zheng, P. N. Prasad, *Chem. Rev.* **2008**, *108*, 1245–1330.
- [3] Z. Feng, T. Tang, T. Wu, X. Yu, Y. Zhang, M. Wang, J. Zheng, Y. Ying, S. Chen, J. Zhou, X. Fan, D. Zhang, S. Li, M. Zhang, J. Qian, *Light: Sci. Appl.* **2021**, *10*, 197.
- [4] P. V. Simpson, L. A. Watson, A. Barlow, G. Wang, M. P. Cifuentes, M. G. Humphrey, *Angew. Chem. Int. Ed.* **2016**, *55*, 2387–2391; *Angew. Chem.* **2016**, *128*, 2433–2437.
- [5] Y. Jiang, K. F. Li, K. Gao, H. Lin, H. L. Tam, Y. Y. Liu, Y. Shu, K. L. Wong, W. Y. Lai, K. W. Cheah, *Angew. Chem. Int. Ed.* **2021**, *60*, 10007–10015; *Angew. Chem.* **2021**, *133*, 10095–10103.
- [6] Q. Zheng, H. Zhu, S.-C. Chen, C. Tang, E. Ma, X. Chen, *Nat. Photonics* **2013**, *7*, 234–239.
- [7] L. Zhang, M. Morshedi, M. G. Humphrey, *Angew. Chem. Int. Ed.* **2022**, *61*, e202116181; *Angew. Chem.* **2022**, *134*, e202116181.
- [8] B. Babgi, L. Rigamonti, M. P. Cifuentes, T. C. Corkery, M. D. Randles, T. Schwich, S. Petrie, R. Stranger, A. Teshome, I. Asselberghs, K. Clays, M. Samoc, M. G. Humphrey, *J. Am. Chem. Soc.* **2009**, *131*, 10293–10307.
- [9] The preparation and properties (particularly photo-electronic and photo-catalytic) of heptazine derivatives and heptazine-based materials have attracted recent interest. See, for example: a) P. Audebert, E. Kroke, C. Posern, S.-H. Lee, *Chem. Rev.* **2021**, *121*, 2515–2544; b) S. Wang, J. Zhang, B. Li, H. Sun, S. Wang, *Energy Fuels* **2021**, *35*, 6504–6526.
- [10] The quadratic optical nonlinearity of 2,5,8-tris(diethylamino)heptazine has been reported: B. Traber, T. Oeser, R. Gleiter, M. Goebel, R. Wortmann, *Eur. J. Org. Chem.* **2004**, 4387–4390.
- [11] A purely theoretical report has appeared: W. Zheng, N.-B. Wong, W.-K. Li, A. Tian, *J. Chem. Theory Comput.* **2006**, *2*, 808–814.
- [12] M. G. Kuzyk, *Phys. Rev. A* **2005**, *72*, 053819.
- [13] J. Pérez-Moreno, M. G. Kuzyk, *Adv. Mater.* **2011**, *23*, 1428–1432.
- [14] T. Schwich, M. P. Cifuentes, P. A. Gugger, M. Samoc, M. G. Humphrey, *Adv. Mater.* **2011**, *23*, 1433–1435.
- [15] Z. Feng, D. Li, M. Zhang, T. Shao, Y. Shen, X. Tian, Q. Zhang, S. Li, J. Wu, Y. Tian, *Chem. Sci.* **2019**, *10*, 7228–7232.
- [16] L. Ravotto, S. L. Meloni, T. V. Esipova, A. E. Masunov, J. M. Anna, S. A. Vinogradov, *J. Phys. Chem. A* **2020**, *124*, 11038–11050.

Manuscript received: June 2, 2022

Accepted manuscript online: July 1, 2022

Version of record online: July 19, 2022